JACS
JOURNAL OF THE AMERICAN CHEMICAL SOCIETY
Article
pubs.acs.org/JACS

Ligand Noninnocence of Thiolate/Disulfide in Dinuclear Copper Complexes: Solvent-Dependent Redox Isomerization and Proton-Coupled Electron Transfer

Andrew M. Thomas,[†,§] Bo-Lin Lin,[†,§] Erik C. Wasinger,[‡] and T. Daniel P. Stack*[,†]

[†]Department of Chemistry, Stanford University, Stanford, California 94305, United States
[‡]Department of Chemistry, California State University Chico, Chico, California 95929, United States

Supporting Information

ABSTRACT: Copper thiolate/disulfide interconversions are related to the functions of several important proteins such as human Sco1, Cu−Zn superoxide dismutase (SOD1), and mammalian zinc-bonded metallothionein. The synthesis and characterization of well-defined synthetic analogues for such interconversions are challenging yet provide important insights into the mechanisms of such redox processes. Solvent-dependent redox isomerization and proton-coupled electron transfer mimicking these interconversions are observed in two structurally related dimeric $\mu,\eta^2:\eta^2$-thiolato Cu(II)Cu(II) complexes by various methods, including X-ray diffraction, XAS, NMR, and UV−vis. Spectroscopic evidence shows that a solvent-dependent equilibrium exists between the dimeric μ-thiolato Cu(II)Cu(II) state and its redox isomeric μ-disulfido Cu(I)Cu(I) form. Complete formation of μ-disulfido Cu(I)Cu(I) complexes, however, only occurs after the addition of 2 equiv of protons, which promote electron transfer from thiolate to Cu(II) and formation of disulfide and Cu(I) via protonation of the coordinating ligand. Proton removal reverses this reaction. The reported unusual reductive protonation/oxidative deprotonation of the metal centers may serve as a new chemical precedent for how related proteins manage Cu ions in living organisms.

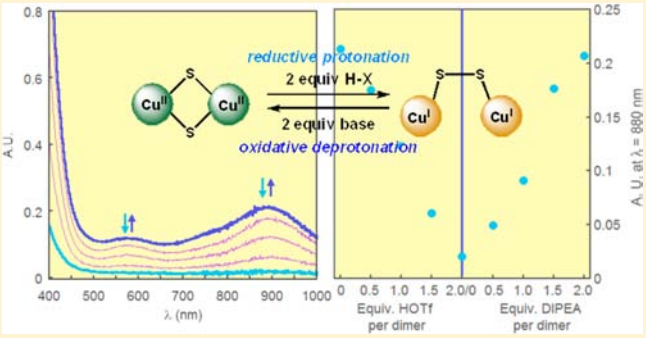

1. INTRODUCTION

Highly specific, sulfur-rich proteins (*e.g.*, Atx1, Cox17, Sco1, CCS, metallothioneins) transport copper (Cu), an essential cofactor for many enzymes, to cellular targets with tight control.[1−10] The most common mechanism of transport is nucleophilic attack by an apoprotein thiol on a S−Cu^{I}−S donor,[11] but a small number of processes may use the redox flexibility of cysteine residues for function.[7,12] For example, a Cu thiolate/disulfide interconversion in human Sco1 is hypothesized as one potential mechanism for Cu delivery to the Cu_A site of cytochrome *c* oxidase.[13−16] Disulfide bond formation is essential for the activity of Cu−Zn superoxide dismutase (SOD1) and is accelerated greatly in the presence of O_2 and Cu−CCS, its copper chaperone, potentially via Cu(II) formed by aerobic oxidation of Cu(I).[8] Cu thiolate/disulfide interconversions may also operate in malfunctioning living systems to prevent aberrant reactive oxygen species (ROS) production by Cu.[17] Mammalian Zn_7MT-3 (zinc-bonded metallothionein) exchanges Zn(II) ions with Cu(II) originating from soluble or aggregated amyloid β peptide (CuAβ). During the process, four cysteine thiolates of Zn_7MT-3 are oxidized by four Cu(II) ions to create four Cu(I) ions and two disulfide bonds along with the release of three Zn(II) ions (Figure 1).[18−20] CuAβ is hypothesized to be a source of ROS production in Alzheimer's disease,[21−23] and this Zn/Cu exchange results in a redox-inactive ZnAβ peptide.

The exact mechanisms of the Cu thiolate/disulfide interconversion exploited by living organisms are not well understood.[25] A possible pathway involving a dimeric dithiolato Cu(II) intermediate was suggested by an early kinetic study of the anaerobic oxidation of 2-mercaptosuccinic acid by Cu(II) perchlorate.[26] The characterization of well-defined, dimeric dithiolato Cu(II) complexes and their interconversions with disulfido Cu(I) complexes provide chemical precedence and mechanistic insights into such a redox process. Two coordination modes of bridging disulfides are known to exist currently: *cis*-μ-disulfido Cu(I)Cu(I) and *trans*-μ-disulfido Cu(I)Cu(I). The complexes can undergo a redox isomerization to the isomeric bis-thiolate species μ-thiolato Cu(II)Cu(II) (Scheme 1). Three examples show that Cu(I) disulfide/Cu(II) thiolate interconversions are induced by either the ligand environment[27] or the coordination of an anionic donor such as chloride.[28,29] Additionally, the subtle shifting of a thiolate/disulfide equilibrium of a coordinatively unsaturated μ-thiolato Cu(II)Cu(II) complex by bonding acetonitrile (MeCN)

Received: September 20, 2013
Published: November 26, 2013

   dx.doi.org/10.1021/ja409603m | *J. Am. Chem. Soc.* 2013, 135, 18912−18919

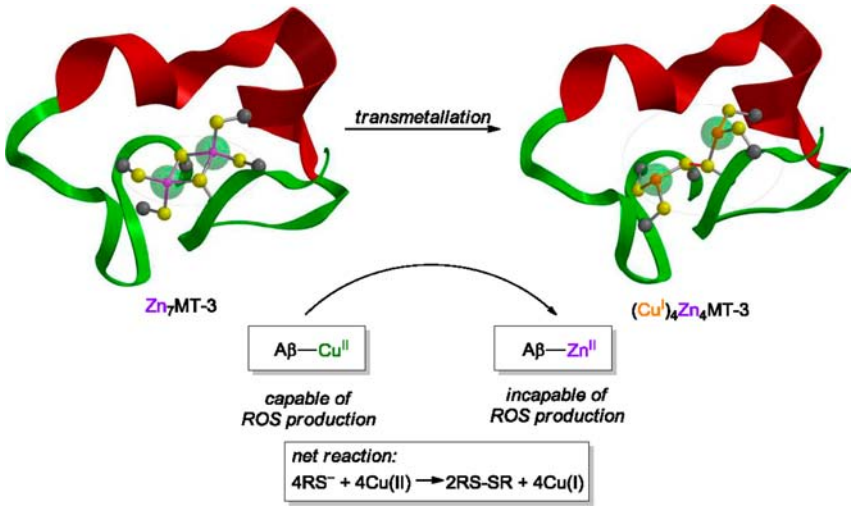

Figure 1. Biological example of a postulated thiolate to disulfide interconversion. This Cu/Zn exchange between a Zn metallothionein (MT) and Cu(II)-bonded amyloid β peptide (CuAβ) results in disulfide bond formation, and the sequestration of Cu by the MT peptide silences ROS production of the Aβ peptide.[18−20] The MT structures are unknown but are represented here for illustrative purposes on the basis of the NMR solution structure of human CdMT-3.[24]

Scheme 1. Examples of Ligand Noninnocence in Dinuclear Copper Disulfide/Thiolate Complexes[a]

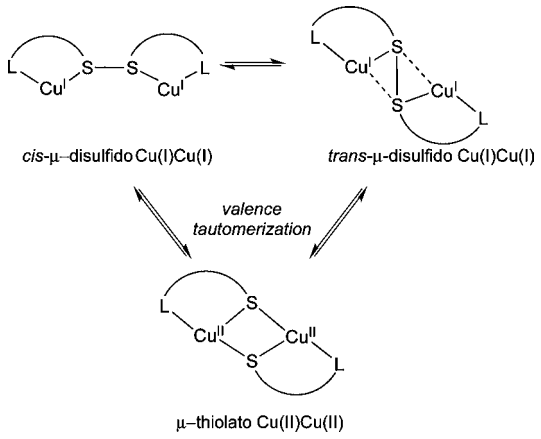

[a]The flexible coordination of a disulfide ligand is represented by geometric, *cis*-μ-disulfido Cu(I)Cu(I) and *trans*-μ-disulfido Cu(I)Cu(I) complexes and a redox isomeric, μ-thiolato Cu(II)Cu(II) species.

solvent has been described briefly by Itoh and co-workers.[30] The scarcity of known examples for the interconversions arises from the difficulty in preparing stable, dimeric Cu(II) thiolate complexes[31,32] as well as the ligand noninnocence and flexible coordination of the resulting disulfide.

Herein, we report that solvent-dependent redox isomerization of μ-thiolato Cu(II)Cu(II) to a μ-disulfido Cu(I)Cu(I) species is a phenomenon more general than previously recognized,[30] and importantly that the Cu(II) thiolate/Cu(I) disulfide interconversion can be controlled completely by simple addition or removal of protons.[33] This report provides the first evidence that the redox isomerization of Cu ligated by sulfur, a ubiquitous motif in bioinorganic chemistry, via proton-coupled electron transfer is a possible mechanism in the transport of Cu in living organisms.[34] In this mechanism, formal reduction/oxidation of the metal centers by protonation/deprotonation of the complexes occurs, which may be classified as hitherto uncharacterized "reductive protonation" and "oxidative deprotonation". These ostensibly unusual phenomena highlight the intricate nature of metal complexes with noninnocent ligands that serve as electron reservoirs during the addition or removal of protons.

2. RESULTS AND ANALYSIS

2.1. Synthesis and Solid-State Characterizations of 1 and 2. The two μ-thiolato Cu(II)Cu(II) complexes **1** (R = Me) and **2**[27] (R = H) were prepared by mixing a 1:2 ratio of the disulfide ligands L^R–L^R with a Cu(I) salt in acetonitrile (MeCN) at room temperature under a N_2 atmosphere (eq 1).

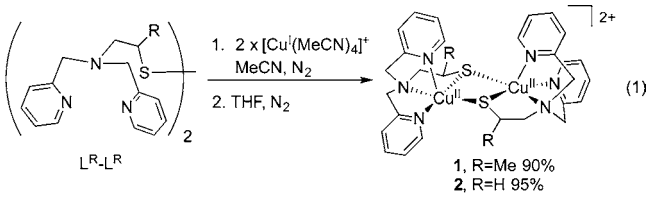

(1)

Addition of tetrahydrofuran (THF) to the resulting solutions precipitated the complexes as dark green, air-sensitive crystalline solids. X-ray crystallography confirmed the dimeric structure of **1** (Figure 2), and the structural parameters are similar to the values of **2** reported by Itoh and co-workers (Table 1).[27] Complexes **1** and **2** exhibit pentacoordinate Cu centers with similar Cu···Cu (2.94 and 2.96 Å, respectively) and S···S (3.13 and 3.18 Å, respectively) distances but vary in τ values[35] (0.44 and 0.35, respectively) and fold angles of the Cu−S butterfly core about the S−S axis (59 and 36°, respectively).

2.2. Spectroscopic Characterization of 1 and 2 in Solution. In solution, the spectroscopic features of **1** and **2** are very solvent dependent. Measurements in less coordinating/polar solvents[36] such as acetone give the most pronounced Cu(II) spectroscopic features, whereas more coordinating/polar solvents such as MeCN attenuate Cu(II) signals.

2.2.1. Cu K-Edge X-ray Absorption Spectroscopy (XAS). The Cu K-edge XANES (X-ray absorption near-edge structure) of a crystalline solid-state sample of **1** exhibits a weak feature at 8978.5 eV, characteristic of a formally forbidden Cu(II) 1s → 3d transition (Figure 3, inset).[37] In acetone or MeCN solution,

dx.doi.org/10.1021/ja409603m | J. Am. Chem. Soc. 2013, 135, 18912−18919

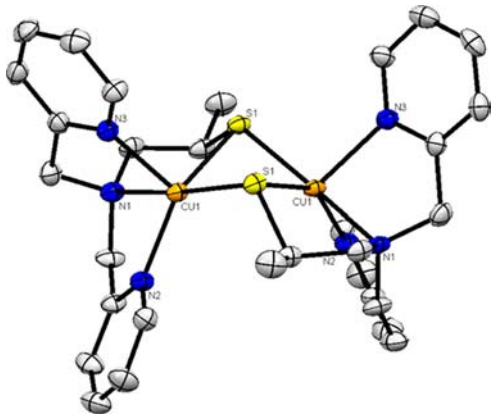

Figure 2. Complex **1**, as determined by X-ray crystallography. Hydrogen atoms, SbF_6 counteranions, and THF solvation molecules are omitted for clarity. This dicationic dimer is 2-fold symmetric. Crystal data for $C_{34}H_{44}Cu_2F_{12}N_6OS_2Sb_2$: monoclinic; space group $C2/c$; a = 21.9655(14) Å; b = 16.3366(14) Å; c = 12.2859(8) Å; β = 97.890(2)°; V = 4367.0(5) Å^3.

Table 1. Selected Bond Lengths and Angles for 1 and 2[a]

	1	2
	Bond Distances (Å)	
Cu−Pyr_{ax}	2.168(3)	2.182(8)
Cu−Pyr_{eq}	2.041(3)	2.018(10)
Cu−N_{sp3}	2.082(3)	2.098(10)
Cu−S	2.2909(8)	2.292(3)
Cu−S′	2.3159(9)	2.303(4)
	Bond Angles (deg)	
Pyr_{eq}−Cu−N_{sp3}	80.45(10)	80.5(4)
Pyr_{eq}-Cu−Pyr_{ax}	105.37(11)	98.4(4)
N_{sp3}−Cu−Pyr_{ax}	80.95(10)	80.2(4)
S−Cu−S′	85.44(3)	87.7(1)
Pyr_{eq}−Cu−S	105.53(8)	102.0(3)

[a]Bond lengths and angles for **2** are reproduced from the initial report by Itoh and coworkers.[27] Abbreviations: Pyr, pyridine; N_{sp3}, tertiary amine; eq, equatorial position; ax, axial position.

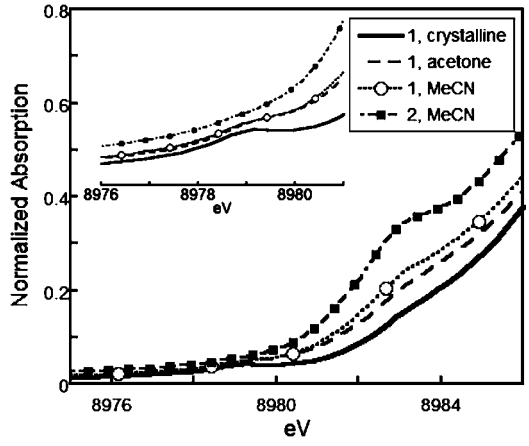

Figure 3. Cu K-edge XAS spectroscopy of crystalline **1** and MeCN solutions (10 mM) of **1** and **2** at 10−15 K. The inset gives the magnified pre-edge region from 8976 to 8981 eV.

this feature is less pronounced with an increase in an 8983 eV feature, characteristic of an electric dipole allowed Cu(I) 1s → 4p transition.[37] In comparison to **1**, an MeCN solution of **2** displays a larger 8983 eV feature with no discernible 8978.5 eV pre-edge feature (Figure 3).

2.2.2. UV−Vis and ^{1}H NMR Spectroscopy. In MeCN, a 0.1 mM solution of **1** shows broad and weak absorption bands in the visible region (λ_{max} 580, 785 nm), as well as a strong feature at 370 nm (Figure 4). Similar but weakened absorption features

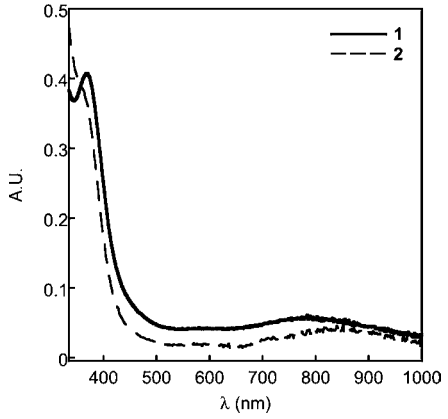

Figure 4. UV−vis spectra of MeCN solutions (0.1 mM, 1 cm path length) of **1** and **2** at room temperature under N_2.

exist for a 0.1 mM solution of **2** in MeCN (λ_{max} 355, 570, 850 nm). In less coordinating/polar solvents (i.e., acetone), significant increases in absorbances in the visible region are observed for **2**. For example, consistent with the initial report of Itoh and co-workers,[27] the UV−vis spectrum of **2** in acetone (λ_{max} 570, 890 nm) shows a 5-fold increase in intensity in the visible region in comparison to that in MeCN (Figure 5). UV−

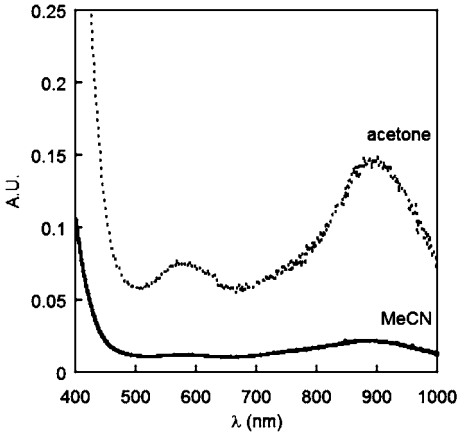

Figure 5. Comparison of UV−vis plots (0.1 mM, 1 cm path length) of **2** in acetone (dashed line) and MeCN (solid line).

vis spectra of **1** in MeCN and acetone show not only differences in intensity but also a shift in the visible λ_{max} absorption by over 150 nm (Figure S3b, Supporting Information).

The ^{1}H nuclear magnetic resonance (NMR) spectrum of **1** (293 K) in d_3-MeCN indicates the presence of a species with paramagnetically broadened features significantly shifted downfield (Figure S4, Supporting Information).[38] In contrast, **2** only contains one set of broad signals in the diamagnetic region at low concentrations in d_3-MeCN (Figure S6a, Supporting Information), consistent with the previous report.[27,39]

dx.doi.org/10.1021/ja409603m | J. Am. Chem. Soc. 2013, 135, 18912−18919

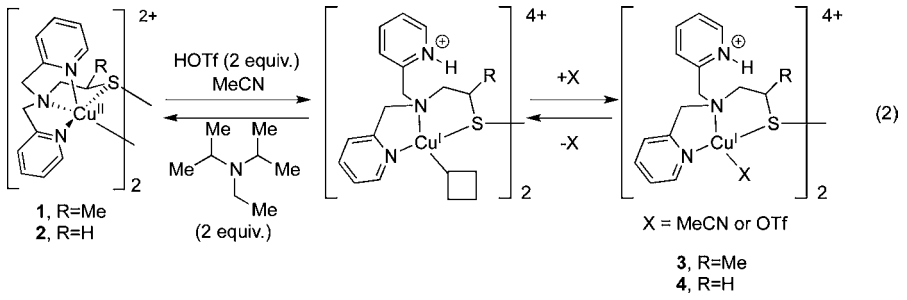

Table 2. Metrical Parameters for Four-Coordinate Cu(I)Cu(I) Disulfide EXAFS Models of 3 and 4 Derived from Cu K-Edge XAS data

	no. of scatters		radius (Å)		σ^2 (Å)^2		F (error)	
vector	3	4	3	4	3	4	3	4
N/O[a]	3	3	1.97	1.97	0.00402	0.00538		
S[a]	1	1	2.23	2.27	0.01295	0.01439		
Cu–N–C (CH_3CN and/or L^R–L^R)[b]	4	4	3.14	3.15	0.00262	0.00418	0.22	0.13
S (distant)[b]	0	1		3.98		0.01162		
Cu–N–C (L^R–L^R)[b]	6	6	4.19	4.32	0.01184	0.01751		
Cu–N–C–C (CH_3CN and/or L^R–L^R)[b]	4	4	4.55	4.56	0.00185	0.00416		

[a]Inner-sphere scatters. [b]Outer-sphere scatters.

2.3. Spectroscopic Characterizations of Proton-Coupled Electron Flow. The addition of 2 equiv of triflic acid (HOTf) to dark green MeCN solutions of **1** and **2** at room temperature under N_2 induces a complete and rapid conversion to the light yellow products **3** and **4**, respectively, assigned as μ-disulfido Cu(I)Cu(I) species (eq 2). Complexes **3** and **4** are O_2-sensitive with limited stability at room temperature. Addition of 2 equiv of diisopropylethylamine (DIPEA) at room temperature induces an instantaneous change back to the spectroscopic signatures attributed to **1** and **2**.

2.3.1. Cu K-Edge XAS. The Cu K-edge spectra of **3** and **4** in MeCN solution have no feature in the 8979 eV region but a rising-edge feature in the 8983–8985 eV range, typical of Cu(I) compounds (Figure S15a–d, Supporting Information). Extended X-ray absorption fine structure (EXAFS) models for **3** and **4** were examined with varying coordination numbers (e.g., N/O_xS_y) in the first coordination sphere (Figure S16 and Tables S5 and S6, Supporting Information) and outer-shell scattering from a linearly bonded CH_3CN, a distant sulfur atom, and/or the ligand framework (e.g., pyridine rings). Invariant in all models is the presence of an ~2.2 Å Cu–S distance and a shell of Cu–N/O distances at ~2.0 Å. Representative distances of EXAFS models for **3** and **4** are shown in Table 2. For **4**, the data are consistent with a model that incorporates one long Cu–S distance (~4 Å), which is much greater than the sum of S and Cu(I) radii of ~2.6 Å[40] and is consistent with a μ-η^1:η^1-disulfido Cu(I)Cu(I) structure. On the basis of EXAFS data alone, N/O_2S_1, N/O_3S_0, and N/O_3S_1 models for both **3** and **4** are valid with similar errors and Debye–Waller factors (σ^2) (Tables S5 and S6, Supporting Information).

2.3.2. UV–Vis and NMR Spectroscopy. Spectroscopic features characteristic of Cu(II) ions for both **1** and **2** are quenched fully upon addition of ≥2 equiv of HOTf in CH_3CN; no evidence of a mixture containing both Cu(II) and Cu(I) is observed. Titration of **2** to **4** with HOTf shows a proportional decay of its absorption features at λ_{max} ~575 and 850 nm and upon the addition of DIPEA re-forms >90% to **2** (Figure 6). Similar behavior was observed by titrating **1** (Figure S8, Supporting Information). The disulfide ligand of **3** (L^H–L^H) is recovered (~75% yield) upon aqueous extraction, characterized by ^{1}H NMR and electrospray ionization mass spectroscopy (ESI-MS) by comparison on authentic sample independently prepared (Figure S19, Supporting Information).

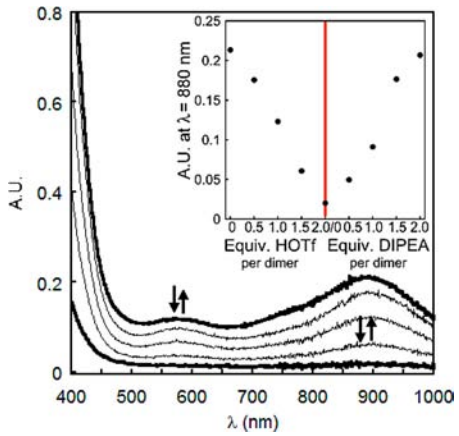

Figure 6. Reversible UV–vis titrations of **2** in CH_3CN (1 mM, 1 cm path length) with triflic acid and diisopropylethylamine. The inset shows changes in absorbance units at 880 nm with the addition of 2 equiv of acid followed by the addition of 2 equiv of base.

Monitoring the titration of **1** to **3** with HOTf by ^{1}H NMR shows paramagnetic to diamagnetic spectral changes (Figure S7a,b, Supporting Information). An additional 1 equiv of HOTf does not significantly alter the NMR spectrum (Figure S9, Supporting Information). Low-temperature (238 K) ^{1}H NMR reveals a broad feature at ~14 ppm, characteristic of a pyridinium proton (Figure S12, Supporting Information); this resonance disappears upon CH_3OD addition (Figure S13, Supporting Information) and exhibits appropriate ^{1}H NOE enhancements to the pyridyl methylene protons of the ligand along with the H_5 and H_6 pyridine protons (Figure S14a,b, Supporting Information). Similar to the reversible behavior of **2**, the addition of DIPEA to complex **3** re-establishes the paramagnetic NMR spectrum of **1** (Figure S9).

dx.doi.org/10.1021/ja409603m | J. Am. Chem. Soc. 2013, 135, 18912–18919

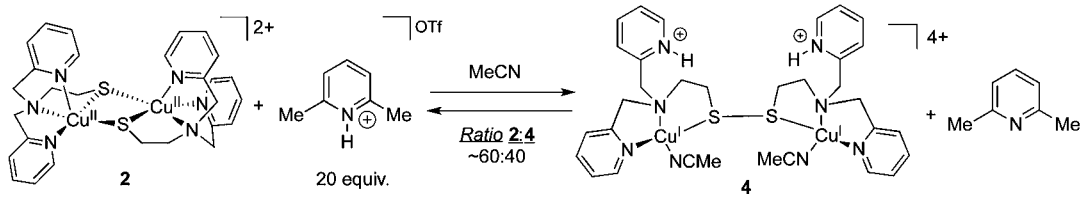

The addition of a weaker acid such as 2,6-lutidinium triflate ([H-Lut]$^+$-OTf) attenuates the 570 and 850 nm optical features of **2**, but only by ca. 20% after the addition of 2 equiv of the acid (Figure S17, Supporting Information). The addition of DIPEA, a stronger base than 2,6-lutidine, results in >90% recovery of **2** (Figure S17). The partial decrease of the Cu(II) features is attributable to the slight acidity of [H-Lut]$^+$-OTf (pK_a = 14.4, CH_3CN; pK_a = 6.8, H_2O).[41] Excess [H-Lut]$^+$-OTf (20 equiv) results in a ∼40% decrease of the 570 and 850 nm features of **2** (eq 3 and Figure S18 Supporting Information).

3. DISCUSSION

3.1. Solvent-Dependent Redox Isomerizations between Cu(II) Thiolate and Cu(I) Disulfide. This work, in combination with the work of Itoh and co-workers,[27] provides crystallographic and Cu K-edge XAS evidence for a μ-thiolato Cu(II)Cu(II) dimeric structure of both **1** and **2** in the solid state. The formation of a μ-thiolato Cu(II)Cu(II) structure for **1** was unexpected, because addition of a Cu(I) salt to the disulfide ligand L^{Me}–L^{Me} was reported recently to yield a μ-disulfido Cu(I)Cu(I) complex (**5^{Me}**; Scheme 2, vide infra) on the basis of its color and mass spectroscopy in MeCN solution.[42,43] The possibility of a μ-thiolato Cu(II)Cu(II) structure, which is indistinguishable from **5^{Me}** by mass spectroscopy, was not discussed. The μ-thiolato Cu(II)Cu(II) form of **1** and **2** results from reduction of the disulfide bond in L^R–L^R upon the coordination of the Cu(I) ions.[44]

Scheme 2. Possible Equilibria of 1 and 2 To Give Structural and Electronic Isomers 5^R and 5^R·solv[a]

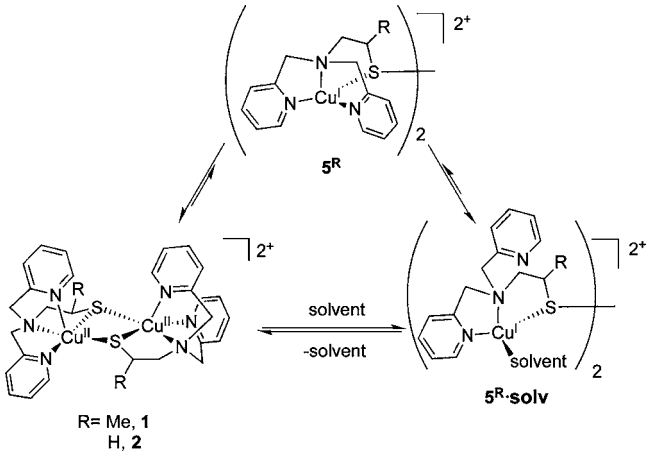

[a]Strongly coordinating solvents such as MeCN favor the Cu(I)Cu(I) disulfide forms of the complexes.

Solutions of **1** and **2** are best interpreted as a mixture of μ-thiolato Cu(II)Cu(II)/μ-disulfido Cu(I)Cu(I) complexes (**1**/**5^{Me}·solv** and **1**/**5^H·solv**, Scheme 2). Five-membered chelate rings, such as N_{sp3}–N_{pyr}–Cu and N_{sp3}–S–Cu in **1** and **2**, preferentially stabilize Cu(II) rather than Cu(I) (e.g., **5^R**), whereas six-membered rings tend to stabilize Cu(I), as evidenced by their more positive Cu(II) reduction potentials.[45,46] With weakly ligating counteranions or solvent, the Cu(II) species should dominate. Ligation of a solvent known to stabilize four-coordinate pseudotetrahedral Cu(I) complexes, such as MeCN, decreases the number of five-membered chelates and apparently shifts the equilibrium toward Cu(I) (**5^R·solv**).

The solvent-dependent redox isomerizations of **1**/**5^{Me}·solv** and **2**/**5^H·solv** provide two examples in addition to the first report of such reactivity by Itoh and co-workers in 2004 (eq 4).[30] No displacement of a nitrogen-ligating subunit is necessary for coordinatively unsaturated complex **6**,[30] but MeCN coordination to each Cu(I) center is proposed to fully bias the equilibrium to the Cu(I) disulfide complex. For **1** or **2**, the competition between solvent bonding and intramolecular pyridine ligation gives rise to equilibrium mixtures of **1** or **2** and **5^R·solv**. While not rigorously quantitative, the relative intensity of the Cu(II) feature, if even present, to the Cu(I) feature qualitatively demonstrates that Cu(I) (**5^R·solv**) is the majority species for **1** and **2** in MeCN and more Cu(I) is present for **1**/**5^{Me}·solv** in MeCN than in acetone, consistent with MeCN being a better ligand for Cu(I) than acetone. In MeCN, **2**/**5^H·solv** has a more dominant 8983 eV feature in comparison to **1**/**5^{Me}·solv**, which presumably obscures the pre-edge Cu(II) feature and possibly explains why UV–vis and NMR of **2**/**5^H·solv** in MeCN appear more Cu(I)-like than **1**/**5^{Me}·solv**.

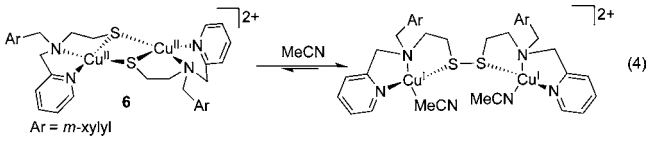

The UV–vis spectra of **1**/**5^{Me}·solv** and **2**/**5^H·solv** in MeCN show optical features consistent with other synthetic N_xS_y bis-thiolato Cu(II) complexes (Table 3) and Cu(II) thiolate proteins Sco and nitrosocyanin—two broad, low-intensity absorbances in the visible region (λ_{max} ∼500–600 and 750–900 nm) and an intense feature in the ultraviolet region (350–380 nm).[47−49] The high-energy feature at 370 nm can be assigned as a $S_{p\sigma}$ → Cu(II) charge transfer (CT), the 500–600 nm feature as a $S_{p\pi}$ → Cu(II) CT, and the broad feature at 750–900 nm as d → d transitions[47] or overlapping signals due to both d → d and a weak $S_{p\pi}$ → Cu(II) CT.[50] The 5-fold decrease in the visible absorption intensities of **2**/**5^H·solv** in MeCN versus those in acetone (Figure 5) corroborates the notion that strongly coordinating solvents stabilize a Cu(I) form of the complex and indicates that a solvated μ-disulfido Cu(I)Cu(I) form dominates in MeCN (>80%).[51] The optical spectra suggest that the concentration of **1** in comparison to **5^{Me}·solv** is greater than the concentration of **2** to **5^H·solv**, which is consistent with the observation of the weak Cu(II) pre-edge feature and less intense Cu(I) edge feature in the XAS for the former (Figure 3). A direct estimation by UV–vis of the

dx.doi.org/10.1021/ja409603m | J. Am. Chem. Soc. 2013, 135, 18912−18919

Table 3. UV−Vis Features of Several Well-Defined Dimeric N_xS_y Cu(II) Complexes

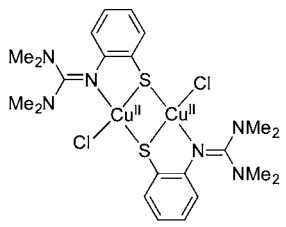

$[Cu_2(NGuaS)_2Cl_2]$

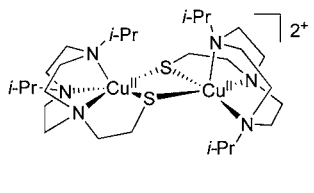

$[L^{N3S}Cu]_2$

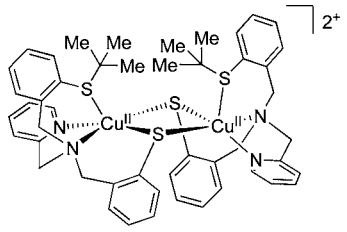

$[Cu_2(N_2SS')_2]$

	1	2	6	$Cu_2(NGuaS)_2Cl_2$	$[L^{N3S}Cu]_2$	$[Cu_2(N_2SS')_2]$
UV−vis (nm)	370, 580, 785 (MeCN)	355, 570, 850 (MeCN)	350, 515, 810 (CH_2Cl_2)	420, 590, 710 (CH_2Cl_2)	340, 380, 675 (MeOH)	350, 590 (CH_2Cl_2)
ref	this work	27, this work	28, 30	29	32a	32c

Scheme 3. Simplest Mechanism for the Formation of 3 or 4 from 1 or 2, Respectively[a]

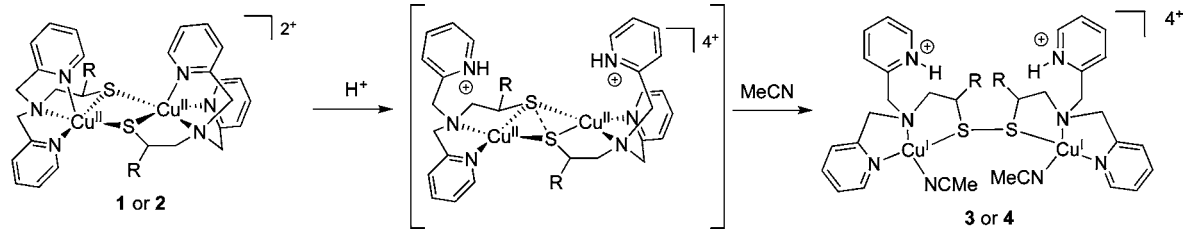

[a]Protonation of a pyridyl ring prevents recoordination and stabilization of the Cu(II) ion.

ratio of **1**:**5**^{Me}**·solv**, however, is complicated by the wide (~150 nm) variation of λ_{max} in the visible window in different solvents.

The ^{1}H NMR signals of **2** in d_3-MeCN are in the diamagnetic region and were attributed originally to an antiferromagentically coupled μ-thiolato Cu(II)Cu(II) dimer.[27] On the basis of the pre-edge XAS (Figure 3) and UV−vis data (Figure 5) presented in this work, we interpret the diamagnetic signals as arising from a Cu(I)Cu(I) complex, which dominates (**5**^{H}**·solv**, >80%). Although similar in structure, **1** shows paramagnetically shifted/broadened resonances in the ^{1}H NMR spectrum in d_3-MeCN (Figure S4, Supporting Information) due to the presence of more Cu(II) than **2**/**5**^{H}**·solv**. The additional methyl groups of L^{Me}−L^{Me} of **2** presumably destabilize the coordination of exogenous solvent ligands and weaken the biasing effect of MeCN on the redox equilibrium.

3.2. Proton-Coupled Electron Transfer. Spectroscopic evidence from UV−vis, XAS, and NMR is consistent with complete formation of **3** and **4** as μ-disulfido Cu(I)Cu(I) complexes with ≥2 equiv of HOTf in CH_3CN. The disappearance of the UV−vis features attributed to the Cu(II) ions in the starting complexes implies indirectly the complete formation of **3** and **4**. Cu K-edge XAS confirms the presence of Cu(I) through the rising-edge features at ~8983 eV. The line shape and intensity of the XAS edge data (Figure S15c,d, Supporting Information) of **4** are characteristic of four-coordinate Cu(I),[37] while those of **3** (Figure S15a,b, Supporting Information) are reminiscent of reduced plastocyanin with a distorted-tetrahedral, four-coordinate Cu(I) center containing a long Cu−S_{Met} bond of ~2.32 Å.[52] As such, the two three-coordinate models (i.e., N/O_2S_1 and N/O_3S_0) are less preferred, even though their EXAFS fits show errors similar to those for the four-coordinate model. EXAFS models support a Cu−S interaction at ~2.3 Å for both **3** and **4**, consistent with the 2.2−2.4 Å Cu−S bond lengths of other η^1-disulfide complexes.[27,29,53−59] The EXAFS models also contain scatters with a focusing effect and enhanced coordination numbers presumably due to a linearly bonded MeCN (Table 2).[60−62] The chemical shift of the exchangeable proton at ~14 ppm in **3** and **4** indicates protonation at the pyridine rather than the amine in each case (e.g., the lutidinium proton of [H-Lut]$^+$-OTf in CD_3CN is ~14 ppm and the ammonium proton of [H-NEt_3]$^+$-OTf is ~7 ppm in CD_3CN), which is further supported by the 1D-NOE ^{1}H NMR enhancements.

The reactivity can be rationalized by initial protonation of axially bonded pyridines (Scheme 3), and complete formation of **3** and **4** ensues after the coordination of acetonitrile in a fashion analogous to eq 4. Upon the protonation and loss of the coordinating pyridine ring, the Cu(II) ions would be more oxidizing, providing a thermodynamic driving force for the oxidation of thiolate to disulfide. The whole process is composed of a sequence of events involving protonation and intramolecular electron transfer. A stepwise protonation of pyridines followed by disulfide formation represents the simplest possibility (Scheme 3), although an alternative mechanism with the redox isomerization occurring immediately after the first protonation cannot be ruled out. The addition of base presumably removes the protons, allowing pyridine ligation to the copper centers, which shifts the equilibrium by reinforcing a Cu(II) stabilizing geometry.

It should be emphasized that strong acids are not necessary to induce this interconversion, as reversible conversions (~20%; Figure S17, Supporting Information) are possible with 2,6-lutidinium triflate (pK_a: 14.0, CH_3CN; 6.8, H_2O).[41] Triflic acid was chosen deliberately to promote thiolate/disulfide interconversion because of the weak coordination of the resulting triflate anions to metals. Strongly coordinative conjugate bases, such as chloride anion, can induce this type of

dx.doi.org/10.1021/ja409603m | J. Am. Chem. Soc. 2013, 135, 18912−18919

redox isomerization through coordination to the metal center.[28,29]

The reversible proton-coupled electron transfer in the interconversions between Cu(II) thiolate and Cu(I) disulfide is unusual, because the addition of protons to transition-metal complexes generally results in either oxidation of the metal center (e.g., $M^n + H^+ \rightarrow [M^{n+2}-H]^+$) or protonation of the ligand (e.g., $M^n-L + H^+ \rightarrow [M^n-LH]^+$), typically not both.[63] In contrast to common electrophilic oxidations of metal centers, the addition of protons to **1** and **2** results in the reduction of the Cu centers. Upon the addition of base and removal of the protons, the Cu centers of **3** and **4** become oxidized. The reverse redox behaviors can be rationalized by synergistic effects of the redox noninnocence of the disulfides to oxidize Cu(I) to Cu(II) and the tendency of Cu(I) to adopt a more stable pseudotetrahedral geometry through loss of a protonated nitrogen ligand and coordination of an exogenous ligand such as solvent.

3.3. Mechanistic Implications of Thiolate/Disulfide Interconversion in Cu Proteins. This work provides the first chemical precedence for a thiolate/disulfide redox isomerization triggered through loss of a coordinating ligand via protonation. Similar mechanisms may be envisioned in thiolate oxidation to disulfide by Cu(II) in Sco proteins,[14] CCS,[8] and Zn_7MT-3.[18−20] For example, the redox behavior of Sco proteins is proposed to be controlled by a histidine "on/off" switch analogous to the work present here; the WT protein with a Cu(II) $His^{135}Cys^{45}Cys^{49}$ coordination environment is redox stable, whereas mutant H135A shows spontaneous oxidation of cysteines to the corresponding disulfide.[64]

4. CONCLUSIONS

The seemingly simple framework of ligands L^R-L^R provides a rich variety of equilibrium processes that involve interplay between the redox-active metal center and the ligands. Solvent-dependent redox isomerization of Cu thiolate/disulfide species is a phenomenon more general than previously recognized. The equilibrium mixture of μ-thiolato Cu(II) and μ-disulfido Cu(I) complexes can be shifted exclusively to Cu(I) products in the presence of protons and be reversed by the addition of base. Proton transfer, in addition to the coordination of solvent, provides the driving force for the electron transfer underlying the interconversions between the two species. The thiolate/disulfide interconversion described here establishes a new chemical precedent for using protons to control both the coordination environment around a Cu center and triggering redox isomerizations in the management of Cu by sulfur-containing proteins. The ease with which thiolates and disulfides interconvert demonstrates that this redox switch may be exquisitely sensitive to subtle changes in chemical environment in living organisms.

■ ASSOCIATED CONTENT

Supporting Information

Text, additional figures, tables, experimental details, and a CIF file for **1**. This material is available free of charge via the Internet at http://pubs.acs.org.

■ AUTHOR INFORMATION

Corresponding Author

stack@stanford.edu

Author Contributions

[§]These authors contributed equally.

Notes

The authors declare no competing financial interest.

■ ACKNOWLEDGMENTS

A.M.T. and B.-L.L. gratefully acknowledge a fellowship award from the Center for Molecular Analysis and Design (CMAD) at Stanford University for the support of this work. We thank Dr. S. Lynch for NMR assistance (Stanford University) and Dr. A. Oliver for X-ray crystallographic assistance (University of Notre Dame). We also thank Drs. C. E. D. Chidsey, Pratik Verma, and Katharina Butsch for helpful discussions during the preparation of the manuscript.

■ REFERENCES

(1) Kim, B.-E.; Nevitt, T.; Thiele, D. J. *Nat. Chem. Biol.* **2008**, *4*, 176−185.

(2) Banci, L.; Bertini, I.; Cantini, F.; Ciofi-Baffoni, S. *Cell. Mol. Life Sci.* **2010**, *67*, 2563−2589.

(3) Arnesano, F.; Banci, L. Copper Transporters and Chaperones. *Encyclopedia of Inorganic and Bioinorganic Chemistry [Online]*; Wiley: Hoboken, NJ, 2011.

(4) Rubino, J. T.; Franz, K. J. *J. Inorg. Biochem.* **2012**, *107*, 129−143.

(5) Robinson, N. J.; Winge, D. R. *Annu. Rev. Biochem.* **2010**, *79*, 537−562.

(6) Boal, A. K.; Rosenzweig, A. C. *Chem. Rev.* **2009**, *109*, 4760−4779.

(7) Lamb, A. L.; Torres, A. S.; O'Halloran, T. V.; Rosenzweig, A. C. *Nat. Struct. Biol.* **2001**, *8*, 751−755.

(8) Furukawa, Y.; Torres, A. S.; O'Halloran, T. V. *EMBO J.* **2004**, *23*, 2872−2881.

(9) Arnesano, F.; Balatri, E.; Banci, L.; Bertini, I.; Winge, D. R. *Structure* **2005**, *13*, 713−722.

(10) Banci, L.; Bertini, I.; Ciofi-Baffoni, S.; Hadjiloi, T.; Martinelli, M.; Palumaa, P. *Proc. Natl. Acad. Sci. U.S.A.* **2008**, *105*, 6803−6808.

(11) Huffman, D. L.; O'Halloran, T. V. *J. Biol. Chem.* **2000**, *275*, 18611−18614.

(12) Palumaa, P.; Kangur, L.; Voronova, A.; Sillard, R. *Biochem. J.* **2004**, *382*, 307−314.

(13) Banci, L.; Bertini, I.; Calderone, V.; Ciofi-Baffoni, S.; Mangani, S.; Martinelli, M.; Palumaa, P.; Wang, S. L. *Proc. Natl. Acad. Sci. U.S.A.* **2006**, *103*, 8595−8600.

(14) Horng, Y.-C.; Leary, S. C.; Cobine, P. A.; Young, F. B. J.; George, G. N.; Shoubridge, E. A.; Winge, D. R. *J. Biol. Chem.* **2005**, *280*, 34113−34122.

(15) Cawthorn, T. R.; Poulsen, B. E.; Davidson, D. E.; Andrews, D.; Hill, B. C. *Biochemistry* **2009**, *48*, 4448−4454.

(16) Although it is known that Sco proteins are important in the synthesis of the Cu_A site of cytrochrome *c* oxidase, debate exists if they function as a metallochaperone or as a redox-active thioredoxin: Banci, L.; Bertini, I.; Cavallaro, G.; Ciofi-Baffoni, S. *FEBS J.* **2011**, *278*, 2244−2262.

(17) Jomova, K.; Valko, M. *Toxicology* **2011**, *283*, 65−87.

(18) Meloni, G.; Faller, P.; Vašák, M. *J. Biol. Chem.* **2007**, *282*, 16068−16078.

(19) Meloni, G.; Sonois, V.; Delaine, T.; Guilloreau, L.; Gillet, A.; Teissié, J.; Faller, P.; Vašák, M. *Nat. Chem. Biol.* **2008**, *4*, 366−372.

(20) Pedersen, J. T.; Hureau, C.; Hemmingsen, L.; Heegaard, N. H. H.; Østergaard, J.; Vašák, M.; Faller, P. *Biochemistry* **2012**, *51*, 1697−1706.

(21) Faller, P.; Hureau, C. *Dalton Trans.* **2009**, 1080−1094.

(22) Rauk, A. *Dalton Trans.* **2008**, 1273−1282.

(23) Benilova, I.; Karran, E.; De Strooper, B. *Nat. Neurosci.* **2012**, *15*, 349−357.

(24) PDB ID: 2FJ4. Wu, H.; Zhang, Q. *Human Metallothionein-3.*; dx.doi.org/10.2210/pdb2fj4/pdb.

(25) Jacob, C.; Giles, G. L.; Giles, N. M.; Sies, H. *Angew. Chem., Int. Ed.* **2003**, *42*, 4742−4758.
(26) Lappin, A. G.; McAuley, A. *J. Chem. Soc., Dalton Trans.* **1978**, 1606−1609.
(27) Itoh, S.; Nagagawa, M.; Fukuzumi, S. *J. Am. Chem. Soc.* **2001**, *123*, 4087−4088.
(28) Ueno, Y.; Tachi, Y.; Itoh, S. *J. Am. Chem. Soc.* **2002**, *124*, 12428−12429.
(29) Neuba, A.; Haase, R.; Meyer-Klaucke, W.; Flörke, U.; Henkel, G. *Angew. Chem., Int. Ed.* **2012**, *51*, 1714−1718.
(30) Osako, T.; Ueno, Y.; Tachi, Y.; Itoh, S. *Inorg. Chem.* **2004**, *43*, 6516−6518.
(31) Mandal, S.; Das, G.; Singh, R.; Shukla, R.; Bharadwaj, P. K. *Coord. Chem. Rev.* **1997**, *160*, 191−235.
(32) Other notable preprations of dimeric Cu(II) thiolate species include the following: (a) Houser, R. P.; Halfen, J. A.; Young, V. G., Jr.; Blackburn, N. J.; Tolman, W. B. *J. Am. Chem. Soc.* **1995**, *117*, 10745−10746. (b) Branscombe, N. D. J.; Blake, A. J.; Marin-Becerra, A.; Li, W.-S.; Parsons, S.; Ruiz-Ramirez, L.; Schröder, M. *Chem. Commun.* **1996**, 2573−2574. (c) Rammal, W.; Belle, C.; Béguin, C.; Duboc, C.; Philouze, C.; Pierre, J.-L.; Le Pape, L.; Bertaina, S.; Saint-Aman, E.; Torelli, S. *Inorg. Chem.* **2006**, *45*, 10355−10362.
(33) Metal thiolate to disulfide formation by the addition of protons has been reported for other metals, although the formal oxidation state of the metal center is not changed in the processes. Mn: Liaw, W.-F.; Hsieh, C.-K.; Lin, G.-Y.; Lee, G.-H. *Inorg. Chem.* **2001**, *40*, 3468−3475. Ru: Tamura, M.; Matsuura, N.; Kawamoto, T.; Konno, T. *Inorg. Chem.* **2007**, *46*, 6834−6836.
(34) Electron transfer from thiolate to an iron center with the concomitant formation of a disulfide bond and reduction of the iron center caused by coordination of exogenous ligands such as CO and trimethyl phosphite was reported recently: Pulukkody, R.; Kyran, S. J.; Bethel, R. D.; Hsieh, C.-H.; Hall, M. B.; Darensbourg, D. J.; Darensbourg, M. Y. *J. Am. Chem. Soc.* **2013**, *135*, 8423−8430.
(35) The τ value is a metric for determining distortion in a five-coordinate species; a square-pyramidal structure has a τ value of 0, while a trigonal-bipyramidal structure has a value of 1.0. See: Addison, A. W.; Rao, T. N.; Reedijk, J.; van Rijn, J.; Verschoor, G. C. *J. Chem. Soc., Dalton Trans.* **1984**, 1349−1356.
(36) Díaz-Torres, R.; Alvarez, S. *Dalton Trans.* **2011**, *40*, 10742−10750.
(37) Kau, L. S.; Spira-Solomon, D. J.; Penner-Hahn, J. E.; Hodgson, K. O.; Solomon, E. I. *J. Am. Chem. Soc.* **1987**, *109*, 6433−6442.
(38) In d_3-MeCN at 293 K the magnetic susceptibility for **1** determined by the Evans method is $\chi_m T = 4.3 \times 10^{-2}$ cm^3 mol^{-1} K, which increases to 1.25×10^{-1} cm^3 mol^{-1} K in d_6-acetone.
(39) At high concentrations in d_3-MeCN at 293 K, the magnetic susceptibility for **2** is $\chi_m T = 2.3 \times 10^{-3}$ cm^3 mol^{-1} K, which increases to 1.6×10^{-1} cm^3 mol^{-1} K in d_2-CH_2Cl_2 and shows paramagnetically broadened signals (Figure S6b, Supporting Information).
(40) Pauling, L. *The Nature of the Chemical Bond*; Cornell University Press: Ithaca, NY, 1945.
(41) Augustin-Nowacka, D.; Chmurzyński, L. *Anal. Chim. Acta* **1999**, *381*, 215−220.
(42) Angamuthu, R.; Byers, P.; Lutz, M.; Spek, A. L.; Bouwman, E. *Science* **2010**, *327*, 313−315.
(43) The addition of $[Cu^I(MeCN)_4]BF_4$ to L^{Me}−L^{Me} is reported to yield a species capable of electrocatalytically coupling two molecules of CO_2 to oxalate. In our hands, we could find no evidence of oxalate formation with complexes **1**−**4** after extensive investigations.
(44) The reduction of a disulfide bond enclosed within a ligand framework has also been reported for mononuclear copper complexes as well: (a) Desbenoît, N.; Galardon, E.; Frapart, Y.; Tomas, A.; Artaud, I. *Inorg. Chem.* **2010**, *49*, 8637−8644. (b) Mandal, S.; Bharadwaj, P. K. *Proc. Indian Acad. Sci. (Chem. Sci.)* **1995**, *107*, 247−254.
(45) Ambundo, E. A.; Deydier, M.-V.; Grall, A. J.; Aguera-Vega, N.; Dressel, L. T.; Cooper, T. H.; Heeg, M. J.; Ochrymowycz, L. A.; Rorabacher, D. B. *Inorg. Chem.* **1999**, *38*, 4233−4242.
(46) Schatz, M.; Becker, M.; Thaler, F.; Hampel, F.; Schindler, S.; Jacobson, R. R.; Tyeklár, Z.; Murthy, N. N.; Ghosh, P.; Chen, Q.; Zubieta, J.; Karlin, K. D. *Inorg. Chem.* **2001**, *40*, 2312−2322.
(47) Basumallick, L.; Sarangi, R.; DeBeer George, S.; Elmore, B.; Hooper, A. B.; Hedman, B.; Hodgson, K. O.; Solomon, E. I. *J. Am. Chem. Soc.* **2005**, *127*, 3531−3544.
(48) Solomon, E. I. *Inorg. Chem.* **2006**, *45*, 8012−8025.
(49) Siluvai, G. S.; Mayfield, M.; Nilges, M. J.; DeBeer George, S.; Blackburn, N. J. *J. Am. Chem. Soc.* **2010**, *132*, 5215−5226.
(50) Holland, P. L.; Tolman, W. B. *J. Am. Chem. Soc.* **1999**, *121*, 7270−7271.
(51) The absorbance and concentration of **2**/$\mathbf{5^H}$**·solv** in acetone were used to calculate the lower bound of the extinction coefficient of **2** in solution. Assuming **2** in acetone and acetonitrile has roughly the same extinction coefficient, the upper bound of the relative amount of **2** was estimated to be 20%.
(52) Solomon, E. I.; Szilagyi, R. K.; DeBeer George, S.; Basumallick, L. *Chem. Rev.* **2004**, *104*, 419−458.
(53) Brändén, C.-I. *Acta Chem. Scand.* **1967**, *21*, 1000−1006.
(54) Ottersen, T.; Warner, L. G.; Seff, K. *J. Chem. Soc., Chem. Commun.* **1973**, 876−877.
(55) Ottersen, T.; Warner, L. G.; Seff, K. *Inorg. Chem.* **1974**, *13*, 1904−1911.
(56) Warner, L. G.; Ottersen, T.; Seff, K. *Inorg. Chem.* **1974**, *13*, 2819−2826.
(57) Carrillo, D. *Coord. Chem. Rev.* **1992**, *119*, 137−169.
(58) Ohta, T.; Tachiyama, T.; Yoshizawa, K.; Yamabe, T.; Uchida, T.; Kitagawa, T. *Inorg. Chem.* **2000**, *39*, 4358−4369.
(59) Ohta, T.; Tachiyama, T.; Yoshizawa, K.; Yamabe, T. *Tetrahedron Lett.* **2000**, *41*, 2581−2585.
(60) Linear molecules such as CH_3CN typically display at least double the coordination numbers in EXAFS models due to the presence of multiple scattering. Multiple scattering originates from the ejected photoelectron wave of Cu traveling to N to C and returning or from Cu directly to C to N and then returning. Additionally, multiple scattering to other parts of the ligand are also observed for complexes **3** and **4**, which gives rise to CN = 4.
(61) Teo, B. K. *J. Am. Chem. Soc.* **1981**, *103*, 3990−4001.
(62) Co, M. S.; Hendrickson, W. A.; Hodgson, K. O.; Doniach, S. *J. Am. Chem. Soc.* **1983**, *105*, 1144−1150.
(63) Hartwig, J. F. *Organotransition Metal Chemistry: From Bonding to Catalysis*; 1st ed.; University Science Books: Sausalito, CA, 2010; Chapters 7.4.2 and 12.
(64) Siluvai, G. S.; Nakano, M. M.; Mayfield, M.; Nilges, M. J.; Blackburn, N. J. *Biochemistry* **2009**, *48*, 12133−12144.